AD A 286541

CONDUCTING THERMOSET POLYMERS

ANNUAL TECHNICAL REPORT

MCDONNELL DOUGLAS

MDC 94X0025
OCTOBER 20, 1994

CONDUCTING THERMOSET POLYMERS
ANNUAL TECHNICAL REPORT

Prepared for
UNITED STATES AIR FORCE
Air Force Office of Scientific Research
Bolling Air Force Base, DC 20332

MCDONNELL DOUGLAS AEROSPACE-EAST

94X0025

REPORT DOCUMENTATION PAGE

Dist: A

Form Approved
OMB No. 0704-0188

1. AGENCY USE ONLY (Leave blank)	2. REPORT DATE	3. REPORT TYPE AND DATES COVERED
	October 1994	Annual Technical Report - 09/30/94

4. TITLE AND SUBTITLE

Conducting Thermoset Polymers

5. FUNDING NUMBERS

61102F 2303 CS

6. AUTHOR(S)

I. M. Brown
D. J. Leopold
T. C. Sandreczki

7. PERFORMING ORGANIZATION NAME(S) AND ADDRESS(ES)

McDonnell Douglas Aerospace-East
P.O. Box 516 MC 1111041
St. Louis, MO 63166-0516

8. PERFORMING ORGANIZATION REPORT NUMBER

MDC 94X0025

AFOSR-TR- 94 07 1 T

9. SPONSORING/MONITORING AGENCY NAME(S) AND ADDRESS(ES)

AFOSR/NCNL
Building 410, Bolling AFB, DC
20332-6448

Dr. Lee

10. SPONSORING/MONITORING AGENCY REPORT NUMBER

F49620-92-C-0074

11. SUPPLEMENTARY NOTES

12a. DISTRIBUTION/AVAILABILITY STATEMENT

APPROVED FOR PUBLIC RELEASE; DISTRIBUTION UNLIMITED.

A

12b. DISTRIBUTION CODE

13. ABSTRACT *(Maximum 200 words)*

Continuing efforts to develop conducting thermoset polymers in which the π-conjugation extends along the backbone and through the crosslink are described. Acetylene-terminated Schiff bases, acetylene-terminated polythiophenes and acetylene-terminated polyanilines are being investigated. Two different approaches to get these thermosets conducting are being pursued: in the AT-Schiff bases and AT-polythiophenes the monomers are first cured then doped with iodine, whereas in the AT-polyanilines the oligomers are first doped with protonic acids then cured. Electron spin resonance, photoluminescence and photo-absorption data suggest that polarons can form in the doped and undoped forms of the AT-Schiff bases and AT-polythiophenes. The dependences of the ESR lineshape parameters of the AT-Schiff bases and amine-cured epoxies on iodine content can be explained in terms of a model involving equilibria between polymeric radical cation complexes containing different stoichiometric amounts of iodine. Several AT-polyaniline oligomers containing either alkoxy substituents or meta substitution in the backbones were synthesized in order to improve the processability of the thermosets. These oligomers were doped with different organic acids. The maximum conductivity value measured was 2×10^{-2} S/cm.

14. SUBJECT TERMS	15. NUMBER OF PAGES
Conducting polymer, thermoset, acetylene-terminated Schiff base, acetylene-terminated polythiophene, acetylene-terminated polyaniline, p-type dopant, acid dopant, electron spin resonance	42
	16. PRICE CODE

17. SECURITY CLASSIFICATION OF REPORT	18. SECURITY CLASSIFICATION OF THIS PAGE	19. SECURITY CLASSIFICATION OF ABSTRACT	20. LIMITATION OF ABSTRACT
UNCLASSIFIED	UNCLASSIFIED	UNCLASSIFIED	

GENERAL INSTRUCTIONS FOR COMPLETING SF 298

The Report Documentation Page (RDP) is used in announcing and cataloging reports. It is important that this information be consistent with the rest of the report, particularly the cover and title page. Instructions for filling in each block of the form follow. It is important to ***stay within the lines*** to meet ***optical scanning requirements***.

Block 1. Agency Use Only (Leave blank).

Block 2. Report Date. Full publication date including day, month, and year, if available (e.g. 1 Jan 88). Must cite at least the year.

Block 3. Type of Report and Dates Covered. State whether report is interim, final, etc. If applicable, enter inclusive report dates (e.g. 10 Jun 87 - 30 Jun 88).

Block 4. Title and Subtitle. A title is taken from the part of the report that provides the most meaningful and complete information. When a report is prepared in more than one volume, repeat the primary title, add volume number, and include subtitle for the specific volume. On classified documents enter the title classification in parentheses.

Block 5. Funding Numbers. To include contract and grant numbers; may include program element number(s), project number(s), task number(s), and work unit number(s). Use the following labels:

C	- Contract	**PR**	- Project
G	- Grant	**TA**	- Task
PE	- Program Element	**WU**	- Work Unit Accession No.

Block 6. Author(s). Name(s) of person(s) responsible for writing the report, performing the research, or credited with the content of the report. If editor or compiler, this should follow the name(s).

Block 7. Performing Organization Name(s) and Address(es). Self-explanatory.

Block 8. Performing Organization Report Number. Enter the unique alphanumeric report number(s) assigned by the organization performing the report.

Block 9. Sponsoring/Monitoring Agency Name(s) and Address(es). Self-explanatory.

Block 10. Sponsoring/Monitoring Agency Report Number. *(If known)*

Block 11. Supplementary Notes. Enter information not included elsewhere such as: Prepared in cooperation with...; Trans. of...; To be published in.... When a report is revised, include a statement whether the new report supersedes or supplements the older report.

Block 12a. Distribution/Availability Statement. Denotes public availability or limitations. Cite any availability to the public. Enter additional limitations or special markings in all capitals (e.g. NOFORN, REL, ITAR).

- **DOD** - See DoDD 5230.24, "Distribution Statements on Technical Documents."
- **DOE** - See authorities.
- **NASA** - See Handbook NHB 2200.2.
- **NTIS** - Leave blank.

Block 12b. Distribution Code.

- **DOD** - Leave blank.
- **DOE** - Enter DOE distribution categories from the Standard Distribution for Unclassified Scientific and Technical Reports.
- **NASA** - Leave blank.
- **NTIS** - Leave blank.

Block 13. Abstract. Include a brief *(Maximum 200 words)* factual summary of the most significant information contained in the report.

Block 14. Subject Terms. Keywords or phrases identifying major subjects in the report.

Block 15. Number of Pages. Enter the total number of pages.

Block 16. Price Code. Enter appropriate price code *(NTIS only)*.

Blocks 17. - 19. Security Classifications. Self-explanatory. Enter U.S. Security Classification in accordance with U.S. Security Regulations (i.e., UNCLASSIFIED). If form contains classified information, stamp classification on the top and bottom of the page.

Block 20. Limitation of Abstract. This block must be completed to assign a limitation to the abstract. Enter either UL (unlimited) or SAR (same as report). An entry in this block is necessary if the abstract is to be limited. If blank, the abstract is assumed to be unlimited.

* U.S.GPO 1990 0 273 271

TABLE OF CONTENTS

LIST OF ILLUSTRATIONS

LIST OF TABLES

LIST OF PAGES

1.0 INTRODUCTION

Our attempts to develop conducting thermoset polymers involve the design of a polymer network where the π-conjugation extends from one end of the sample to the other. For this conjugated network to be one giant molecule the π-conjugation has to extend along the backbone and through the crosslink. Since it has been established[1] that polyene crosslinks form when acetylene-terminated oligomers polymerize, we have chosen to study acetylene-terminated Schiff bases (AT-Schiff bases), acetylene-terminated polyanilines (AT-polyanilines, ATPA) and acetylene terminated polythiophenes (AT-polythiophenes). During this year, the second of our studies, we have also included measurements on several non-conjugated thermosets for comparison purposes. These non-conjugated polymers, which included an epoxy-terminated Schiff base (ET-Schiff base), a vinyl-terminated Schiff base (VT-Schiff base), as well as two amine-cured epoxies, could also be made conducting.

2.0 RESEARCH OBJECTIVE AND APPROACH

Our long range objective is to study the feasibility of using acetylene-termination chemistry to provide the necessary (a) processing, (b) mechanical properties, and (c) electrical conductivity, in a single component conductive thermoset system.

Our approach has been to synthesize selected monomers, hot-melt process these monomers into thermosets and use different doping methods to get them conducting. In the case of the AT-Schiff bases and the AT-polythiophenes the monomers were cured first then doped with iodine. On the other hand, for the AT-polyanilines the oligomers were doped first with protonic acids then cured.

3.0 RESULTS

3.1 AT-Schiff Base and AT-Polythiophene Studies

3.1.1 Electrical Measurements

We have completed a comparative study of the conductivities exhibited by five different thermosets after iodine doping.[2] The structures of the five Schiff base monomers used are

shown in Figure 1. New data on CD-EB and VT-Schiff base has been added to the preliminary data reported previously.[3]

a) 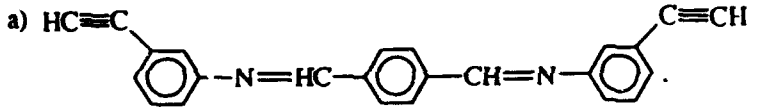

AT-SB

b) 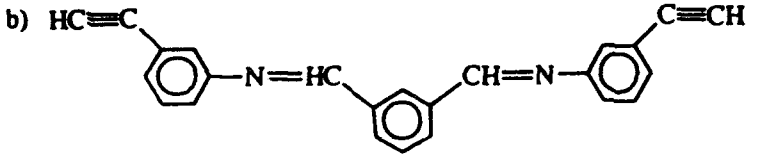

AT-SB

c) 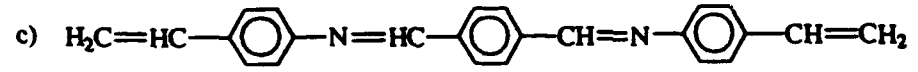

VT-SB

d) 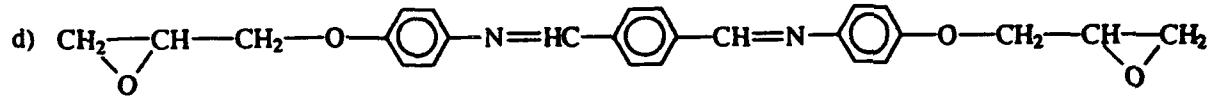

ET-SB

e) 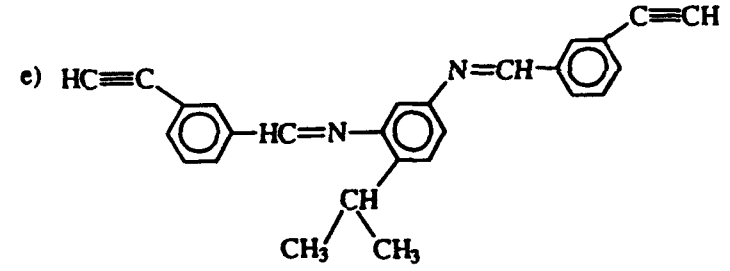

CD-EB

Figure 1. The Schiff base monomers studied: (a) Thermcon 1000, (b) Thermcon 2000, (c) Vinyl-terminated Schiff base, (d) Epoxy-terminated Schiff base, and (e) the Acetylene-terminated Schiff base CD-EB.

The iodine penetration depths were measured from scanning electron micrographs. Knowing the iodine penetration depths allows us to calculate the iodine concentration as well as obtain a measure of the conductivities at different depths into the polymer samples. The data show:

(a) the penetration depth is linearly dependent on the iodine uptake for all four samples,

(b) the iodine concentration is approximately constant at different depths into the polymer with an average value of approximately 2.75 g/cm^3 for all four samples,

(c) the conductivities for the AT-Schiff base thermoset (Thermcon 1000) are constant with increasing depth, and

(d) the conductivities of the ET-Schiff base, VT-Schiff base and CD-EB thermosets appear to increase over the depths measured (in several repeated measurements this was a consistent finding).

If the conductivity depends only on the iodine concentration one would expect the values to be constant with increasing depth, as indeed was observed with the Thermcon 1000 thermoset. The increase in conductivity with increasing depth for the ET-, VT-Schiff base and CD-EB thermosets is possibly the result of microcracking in or adjacent to the conducting layer which is the result of swelling stresses set up in the conducting layer because of the iodine uptake. Furthermore, it is reasonable to expect that such microcracking will play a more decisive role in increasing resistances in the thinner layers. The higher conductivity values for the Thermcon 1000 Schiff base thermoset following iodine doping suggests that the extended conjugation provided by the polyene crosslinks is responsible for the enhanced conductivity. Introduction of the bulky cumyl group as a sidechain in the CD-EB Schiff base thermoset also produces a lowering of the conductivity value over that exhibited by the Thermcon 1000 thermoset. Thus, we have been able to change the conductivities of the Schiff base thermosets by changing the nature of either the crosslink or the backbone.

We have also obtained measurable conductivities in amine-cured epoxy thermosets which are non-conjugated. These included the diglycidyl ether of bisphenol A (DGEBA) cured with stoichiometric amounts of diethylenetriamine (DETA). The structures of these compounds are shown in Figure 2. Measurements of the surface resistivity versus iodine uptake are shown in Figure 3 along with measurements for the ET-Schiff base and Thermcon 1000 thermosets for comparison. The data show that at the same iodine contents the resistivity values for the DGEBA/DETA and the ET-Schiff base thermosets are the same.

a) 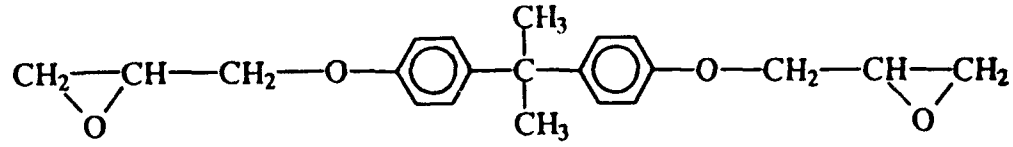

DGEBA

b) 

DETA

c) 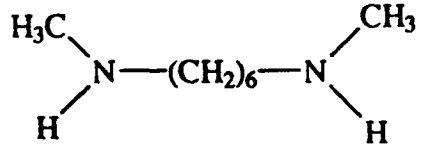

DDH

Figure 2. The epoxy and curing agents studied: (a) the diglycidyl ether of bisphenol A (DGEBA), (b) diethylenetriamine (DETA), and (c) N,N'-dimethyl-1,6-diaminohexane (DDH).

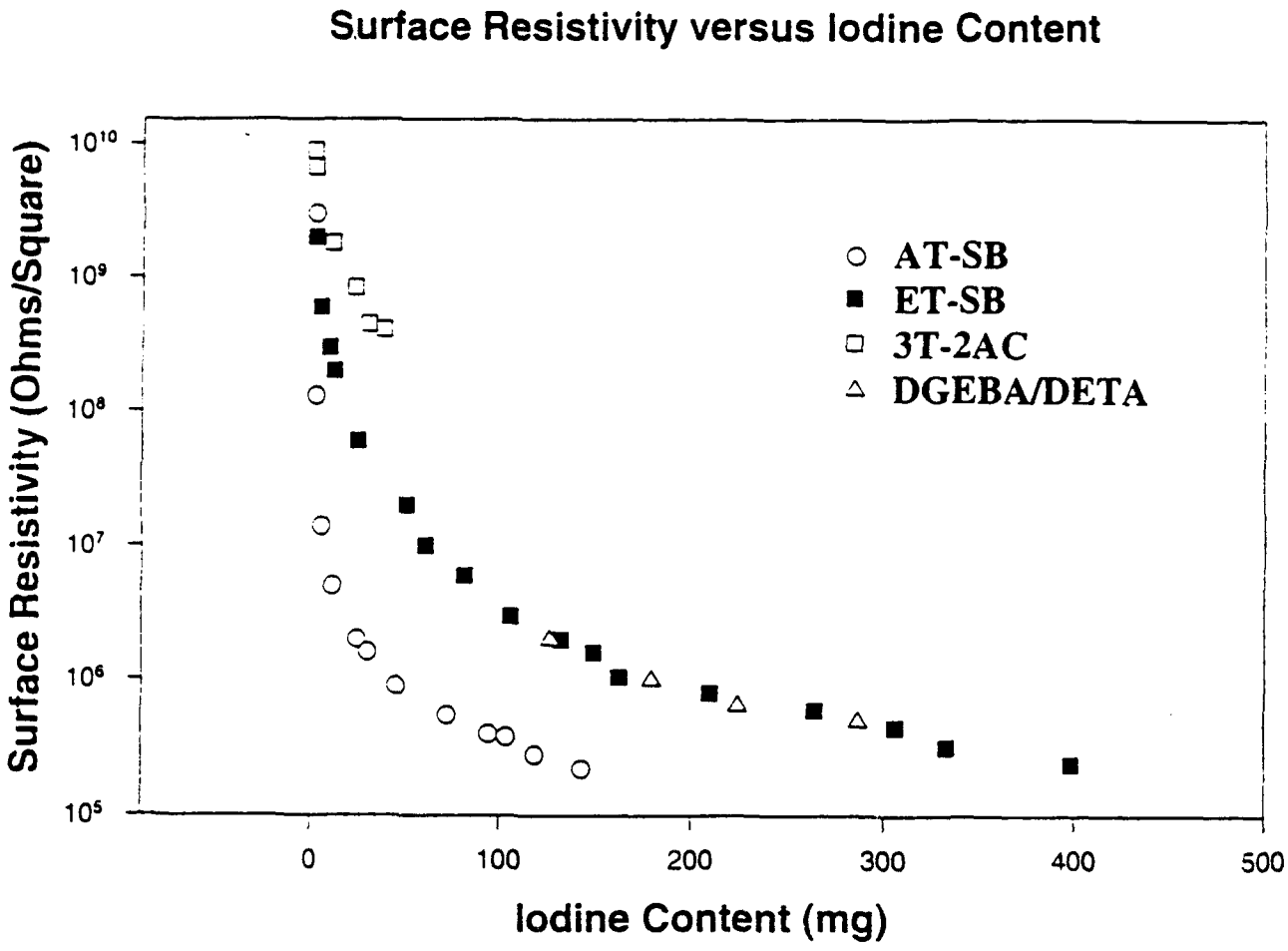

Figure 3 Plots of the surface resistivity versus iodine content for the thermosets studied.

We have also extended our investigations to AT-polythiophenes. The structures of the four polythiophenes being studied are shown in Figure 4. All four have been synthesized in small quantities but electrical measurements are still in progress. To date, we have found that:

T-Si-T-2AC is a volatile liquid which could not be cured into the form of thick films or pellets for accurate electrical measurements. Thin films were cast between glass plates for the optical studies described below.

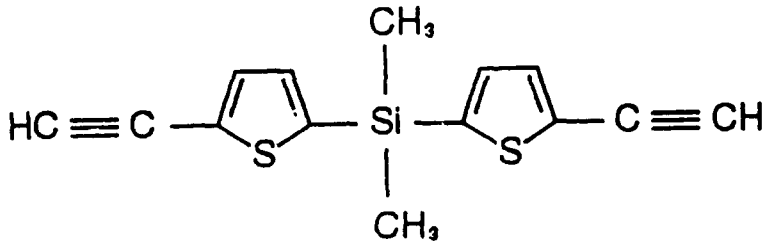

T-Si-T-2AC

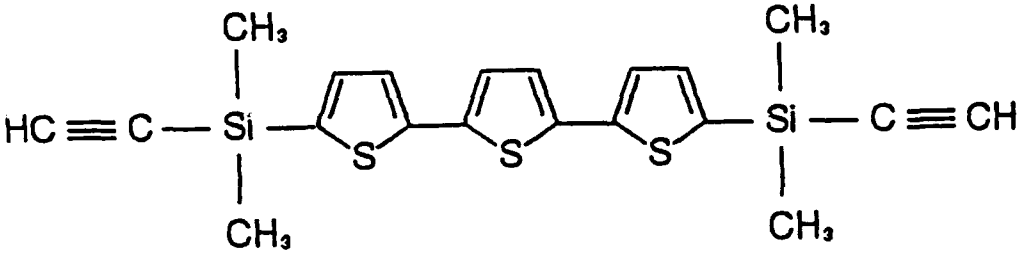

3T-2Si-2AC

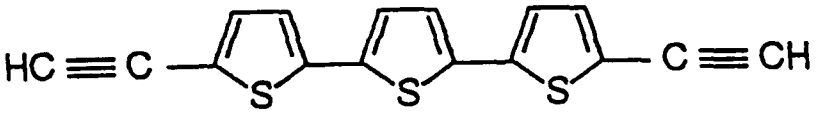

3T-2AC

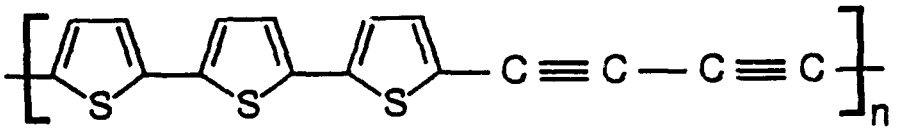

Poly(3T-2AC)

Figure 4. The polythiophenes synthesized and under study.

The DSC for 3T-2AC showed an exotherm at 100°C but no endotherm associated with a melting. The TGA in air showed a weight increase up to 350°C (a maximum increase of 4%) probably due to an air oxidation. Curing at temperatures much above 125°C in air resulted in sample decomposition presumably because of thermal runaway. Pellets of the powder were therefore cured in vacuum oven at 95°C. The mechanical properties of these thermoset samples were poor and as a result only small amounts of iodine could be introduced into the pellet samples before they fell apart because of the swelling caused by the iodine. The measured values of the surface resistivities are shown in Figure 3. The maximum penetration depth was 30 microns giving a maximum conductivity of only 3×10^{-6} S/cm. A high crosslink density, which is a consequence of the short length of the 3T-2AC monomer, may be the reason for the poor mechanical properties. These results illustrate the importance of the mechanical properties in allowing the uptake of the dopant required for high conductivity in thermosets.

3.1.2 Synthesis of Monomers and Oligomers

The three monomers and one oligomer synthesized in the past year for our AT-polythiophene studies are shown in Figure 4. We chose the repeat unit in each compound to contain three thiophene rings since there are reports[4] in the literature that three is the minimum for electrical conduction. Synthesis of repeat units with greater than three (e.g., six) thiophene rings was not pursued since the processing parameters for these materials, such as the melting point and cure temperatures, were likely to be above 250°C. The synthesis for 3T-2AC is outlined[5] in Scheme 1 shown in Figure 5. The synthesis for all four compounds involved multistep preparations, and purification at each step was necessary. All monomers were obtained in good overall yields from a sequence of lithiation, bromination, ethynylation and deprotection. The lithiation was achieved in hexane, and the condensation was carried out by the slow addition of the required chlorosilane. A mild brominating agent such as N-bromosuccinimide (NBS) was

SCHEME I:

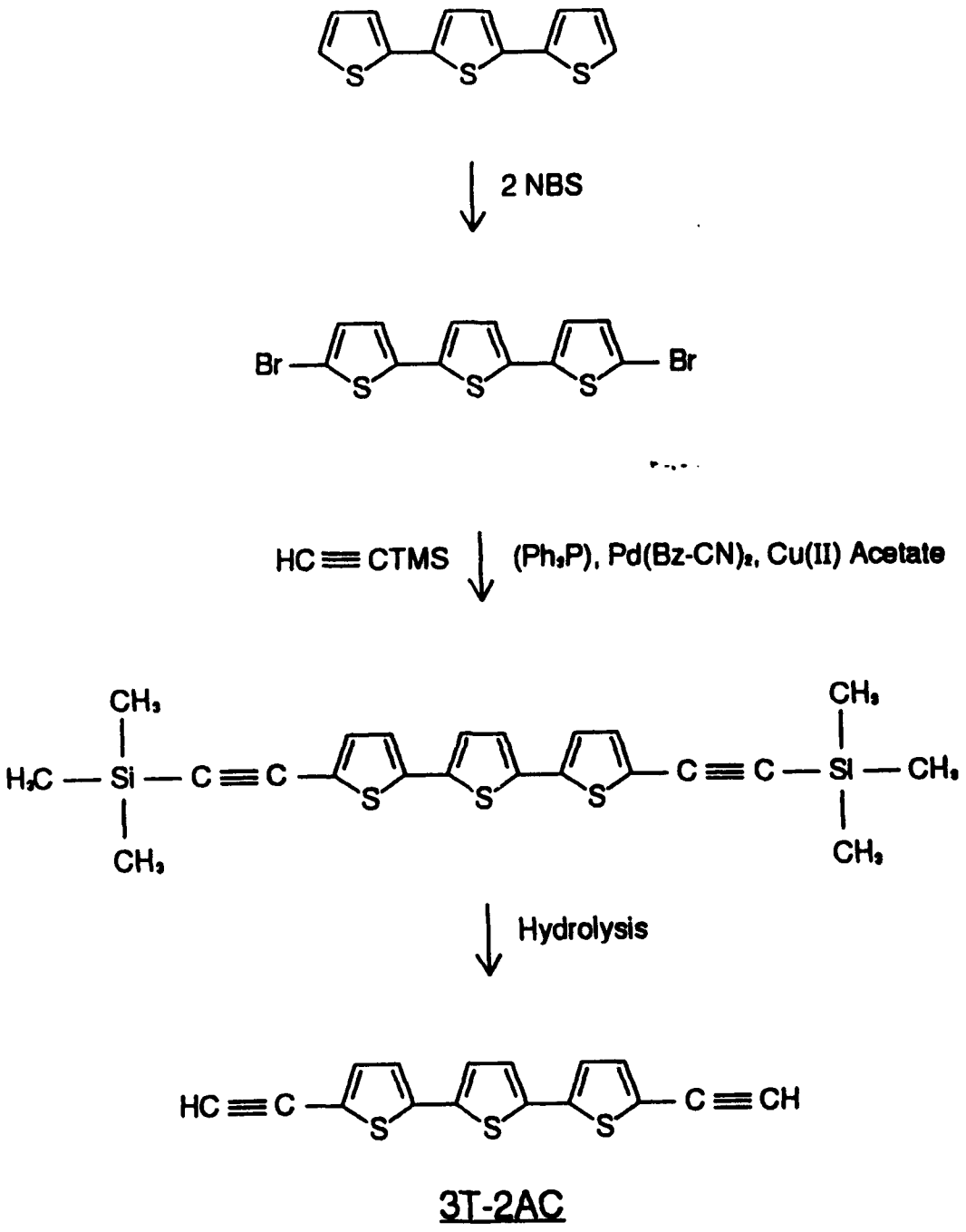

3T-2AC

Figure 5. The preparative scheme used to synthesize 3T-2AC.

used for bromination. Treatment of dibromo compounds with trimethylsilylacetylene (TMS-acetylene) in the presence of palladium in an amine solvent yielded TMS-ethynyl-substituted thiophenes. The TMS protecting groups were removed by hydrolysis with a mild base. All compounds were characterized by elemental analysis, as well as IR and NMR spectroscopy. The polymer shown in Figure 4 containing the acetylene groups in the main chain was prepared as the result of an oxidative polymerization of 3T-2AC which was carried out by the treatment of a solution of the monomer in pyridine and N,N-dimethylformamide (DMF) with copper (I) chloride and oxygen.

3.1.3 Optical Studies

The change in the absorbances of the infrared modes at 3295 cm^{-1} and 2108 cm^{-1} are indicators of the extent of cure in the AT-polythiophene thermosets (just as they were in the AT-Schiff base thermosets reported previously[3]). For example, in the case of 3T-2AC the absorbance peak associated with the C-H stretch mode of acetylene (3295 cm^{-1}) and the absorbance peak associated with the stretch mode of acetylenic carbons (2108 cm^{-1}) become measurably less intense after a 19 h cure at 95°C. This infrared spectral information reassured us that extensive crosslinking had taken place in 3T-2AC prior to our iodine doping studies.

Optical absorption measurements have also provided information on changes in band structure and the creation of states within the gap. In particular, we have measured optical absorptions through thin conductive thermoset polymer films in the visible and infrared regions of the spectrum to determine where oscillator strength changes occur, and if polarons form. We have found that the band-edge of the absorption spectra in thin films of AT-polythiophenes thermosets becomes slightly red-shifted with increasing cure. This observed red shift is attributed to extensive crosslinking, reflecting the transition from a quasi-one-dimensional structure with weak transverse polymer chain coupling to a more three-dimensional crosslinked network structure expected in thermosets. Similar results were reported previously[3] for the AT-Schiff base thermosets.

Iodine doping in AT-polythiophenes produced optical absorption changes involving transitions associated with the band edge and the gap states. For example, Figure 6 shows the absorbance spectra of T-Si-T-2AC films before and after iodine doping. The absorption edge near 500 nm is shifted to longer wavelengths with increasing iodine concentration and an additional absorption peak near 730 nm is observed. This absorbance peak is attributed to polaron formation.

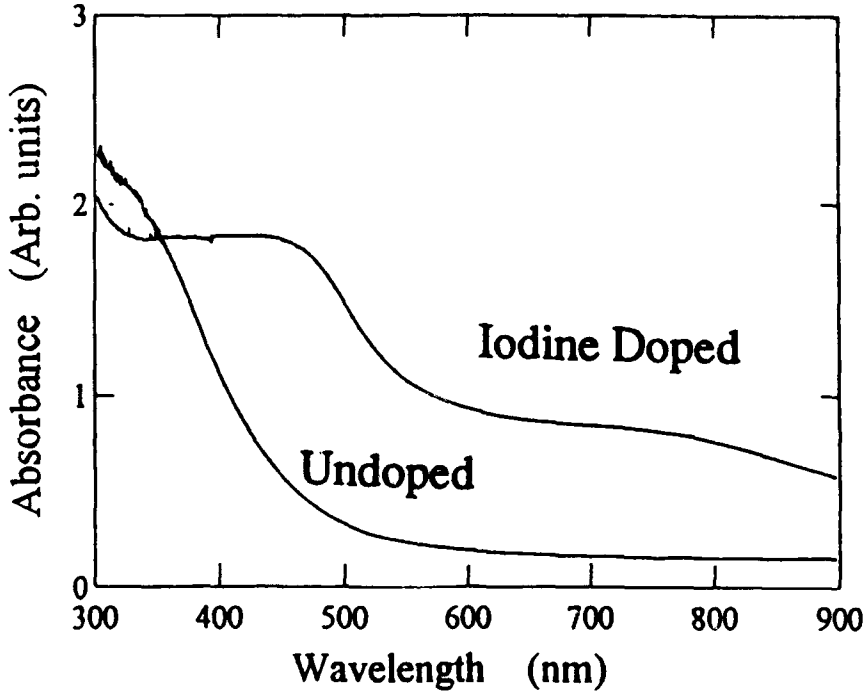

Figure 6. The optical absorption spectra for undoped and iodine doped T-Si-T-2AC.

A low energy shoulder in the photoluminescence spectra is also evidence for polaron formation in both undoped AT-Schiff base and AT-polythiophene thermosets. A typical example of the photoluminescence spectra is shown in Figure 7. This low energy shoulder observed at 1.7 eV (730 nm) coincides with the absorption peak measured in the iodine-doped AT-thermosets. In undoped materials a fraction of the photoexcited charges form polaron states before recombining radiatively at 1.7 eV. As expected, this transition appeared below the band edge energy associated with both thermosets.

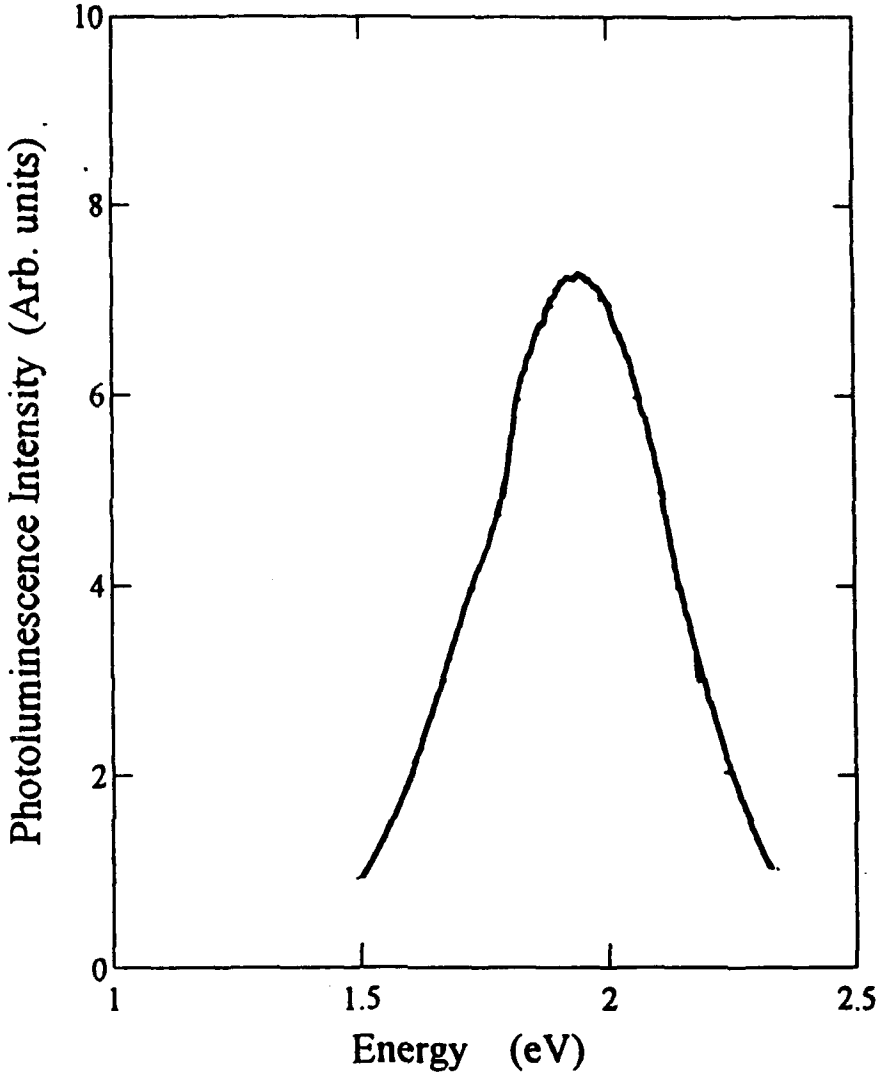

Figure 7. The photoluminescence spectra for T-Si-T-2AC.

Photoluminescence provides information on radiative and nonradiative recombination channels, charge carrier lifetimes, and possible defect trapping states near the band edges in the thermoset polymers. For example, in several AT-thermoset polymers we have found that the photoluminescence intensity decays with time. The decay and recovery times are on the order of minutes and are nonexponential in all materials studied. A likely cause for this behavior is charge trapped on the polymer chain, probably at defects or impurities. The presence of charged

defects can cause a reduction in the observed luminescence response since additional photoexcited charge carriers trapped near these centers decay nonradiatively. When samples remained in the dark for a period of time the trapped charges were released by thermal excitation and there was a subsequent increase in luminescence efficiency.

3.1.4 ESR Results

Detailed ESR studies were carried out on the polymerization process of several monomers as well as the iodine doping process in several thermosets.

Dependence on Polymerization Process: In the polymerization reactions the magnetic susceptibility (i.e., the total spin concentration) was measured as a function of cure time. The thermosets studied were cured samples of Thermcon 1000, the epoxy-terminated Schiff base (ET-SB), the acetylene-terminated terthiophene (3T-2AC) and the diglycidyl ether of bisphenol A. The latter was cured at room temperature with diethylenetriamine (DGEBA/DETA) or N,N'-dimethyl-1,6-diaminohexane (DGEBA/DDH). The structures of these monomers are shown in Figure 2.

The behavior of the magnetic susceptibilities as a function of cure time for the Thermcon 1000 and ET-SB are essentially the same although the mechanism for the changes are different. In the former, the radicals that participate in the cure are trapped in the rigid matrix beyond the gel point.[6] In the latter only radicals formed as a result of thermo-oxidative degradation are trapped in the rigid matrix since the cross-linking of the epoxy end groups with the amine is a nucleophilic (S_N2) reaction, i.e., a non-radical reaction. Thus, thermo-oxidative reactions have to be considered in any evalution of the doped conducting forms of these thermosets. No radicals were detected in the DGEBA/DETA sample cured at room temperature.

Dependence on Iodine Content at Room Temperature: In the iodine doping experiments the line shape parameters, viz., the linewidth (ΔH), the asymmetry parameter (A/B), and the effective g-value (<g>), as well as the magnetic susceptibility, were measured as a function of iodine content ion in samples of both Thermcon 1000 and DGEBA/DETA epoxy. Definitions of the lineshape parameters, <g>, A/B and ΔH, are shown in Figure 8.

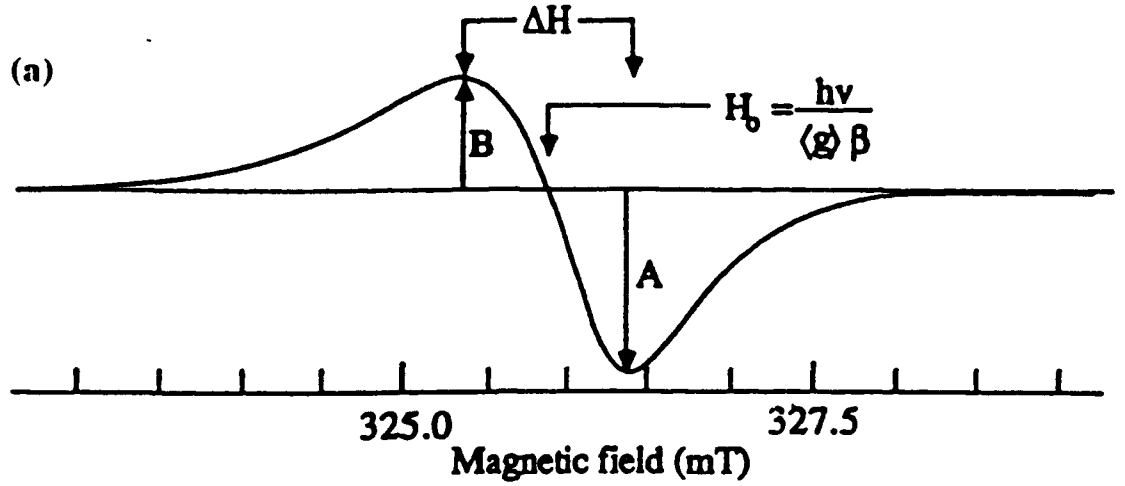

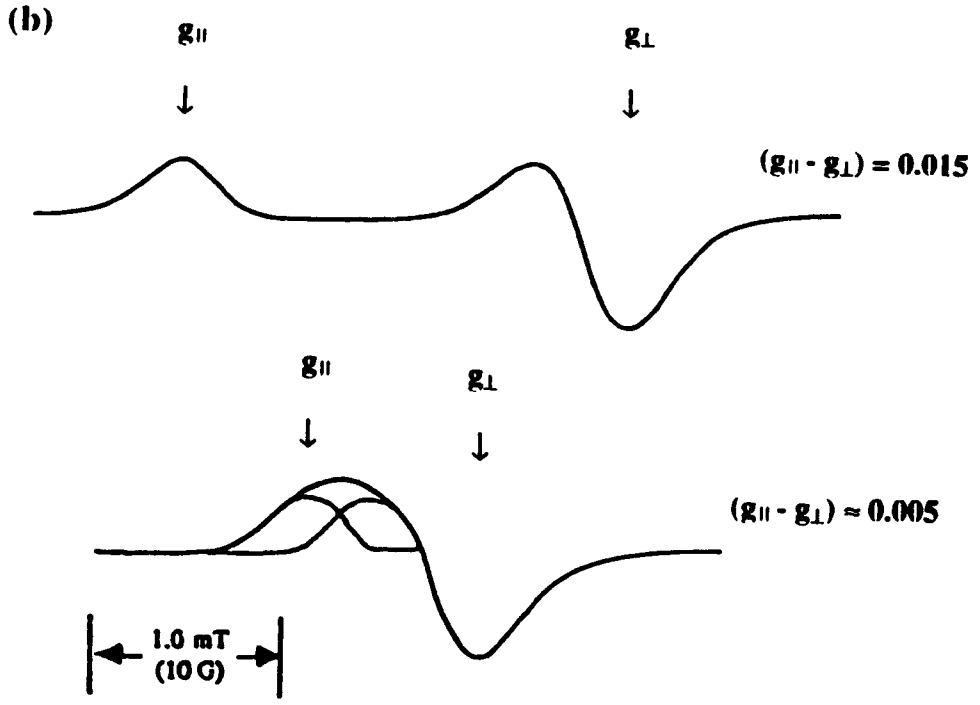

Figure 8. (a) Definition of the ESR lineshape parameters and effective g-value, and (b) an illustration of how g-anisotropy can explain the observed asymmetric lineshape.

As is described above, before iodine doping Thermcon 1000 samples contain a relatively large concentration of radicals which are the result of radicals produced in the radical crosslinking reaction being trapped in the rigid matrix. In evaluating our previously reported results[3] on iodine doping it was not clear how the behavior of these radicals could be distinguished from that of the radicals generated as a result of the redox reaction with iodine as an electron acceptor. We have therefore carried out some new comparative ESR studies of cured samples of Thermcon 1000 and DGEBA/DETA epoxy that have been doped with iodine, since the latter thermoset contains no background ESR line. Figures 9, 10, 11 and 12 show the behavior of the magnetic susceptibilities, the <g>, A/B and ΔH values for the Thermcon 1000 samples, respectively.

As can be seen from this data the magnetic susceptibility and lineshape parameters show some reversible and some irreversible changes as iodine is both added and removed from the samples. All the reversible changes can be explained in terms of the equilibria scheme model shown in Figure 13. For this scheme we have assumed that two types of radical cations can form as a result of oxidation of the polymer by the iodine: viz., the singly charged cation which is paramagnetic (S = 1/2), and the doubly charged cation which is diamagnetic (S = 0). In solid state terminology these species would correspond to a polaron and bipolaron, respectively. The equilibria scheme in Figure 13 also includes the possibility that these cations can exist in different stoichiometric forms. The examples shown in Figure 13 include the charge compensating species I_3^- and I_5^-.

On the first addition of iodine, the radical concentration in both Thermcon 1000 and DGEBA/DETA samples increases with increasing iodine content indicating the formation of radicals by way of the redox reaction with iodine. In the case of the DGEBA/DETA sample, the removal and addition of iodine shows that this radical formation is reversible. On the other hand, in the case of Thermcon 1000 with the first removal of iodine the radical concentration remains high, and in fact increases slightly with decreasing iodine content. However, following the first removal of iodine subsequent additions and removals shows that the formation of radicals is

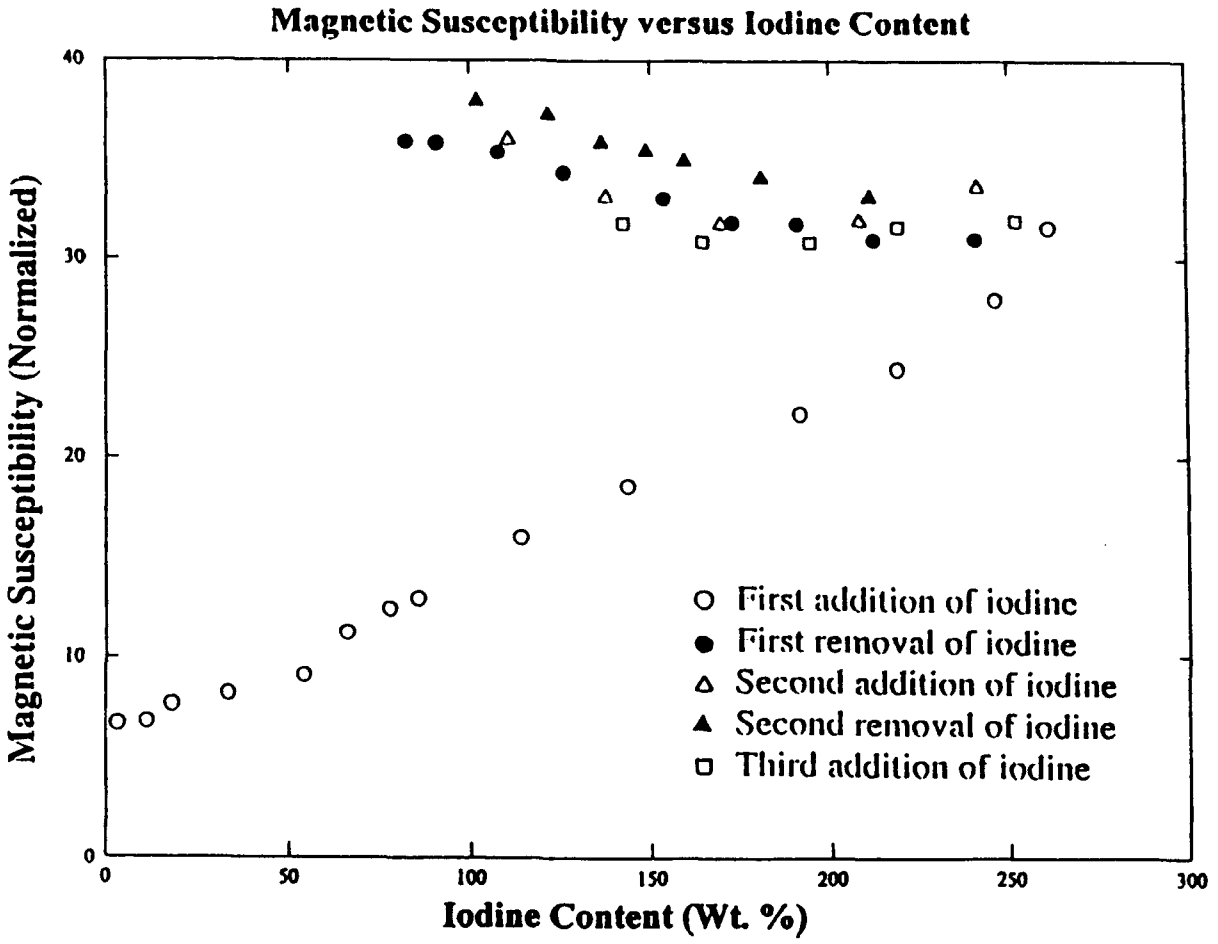

Figure 9. A plot of the magnetic susceptibility versus iodine content for Thermcon 1000.

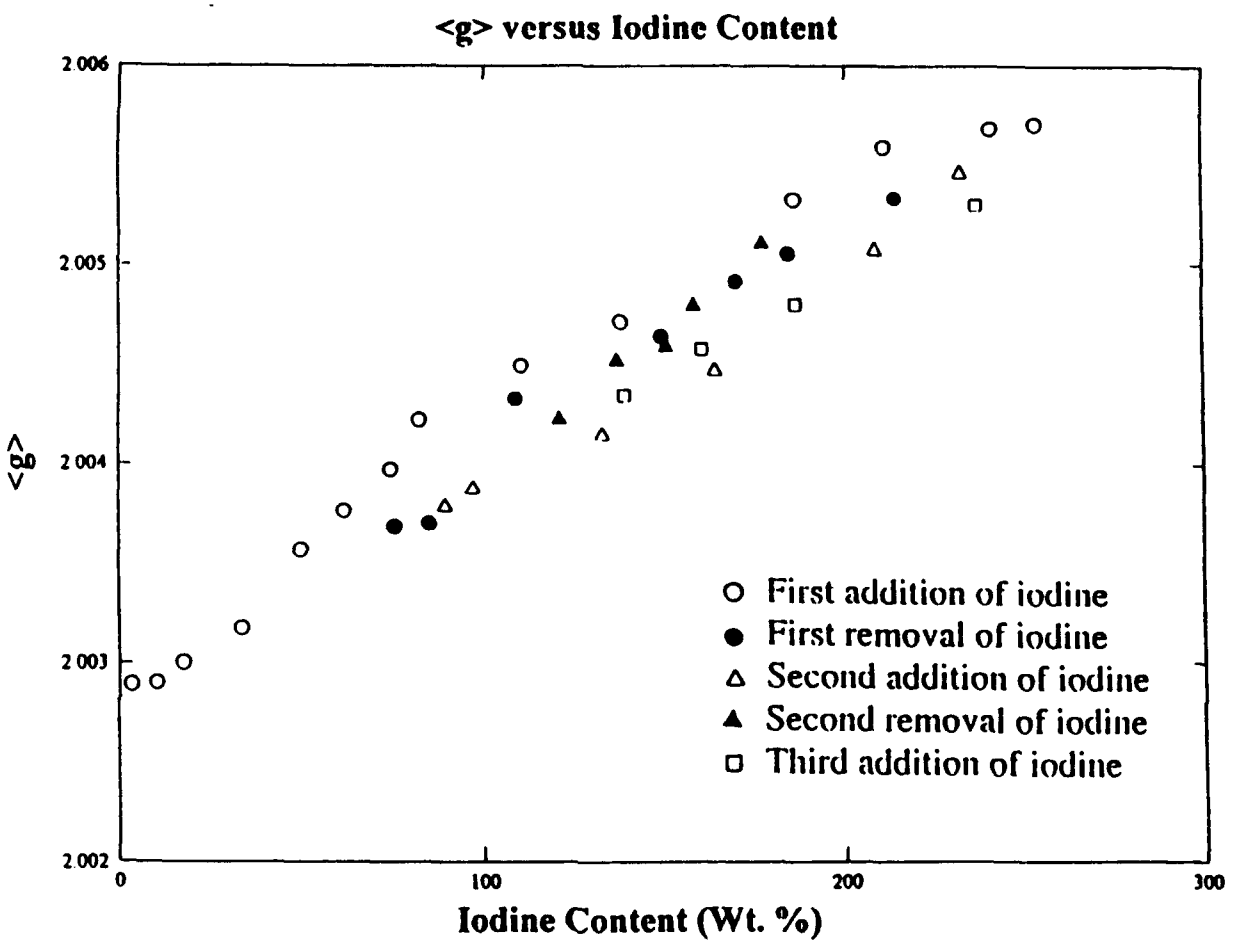

Figure 10. A plot of effective g-value, <g>, versus iodine content for Thermcon 1000.

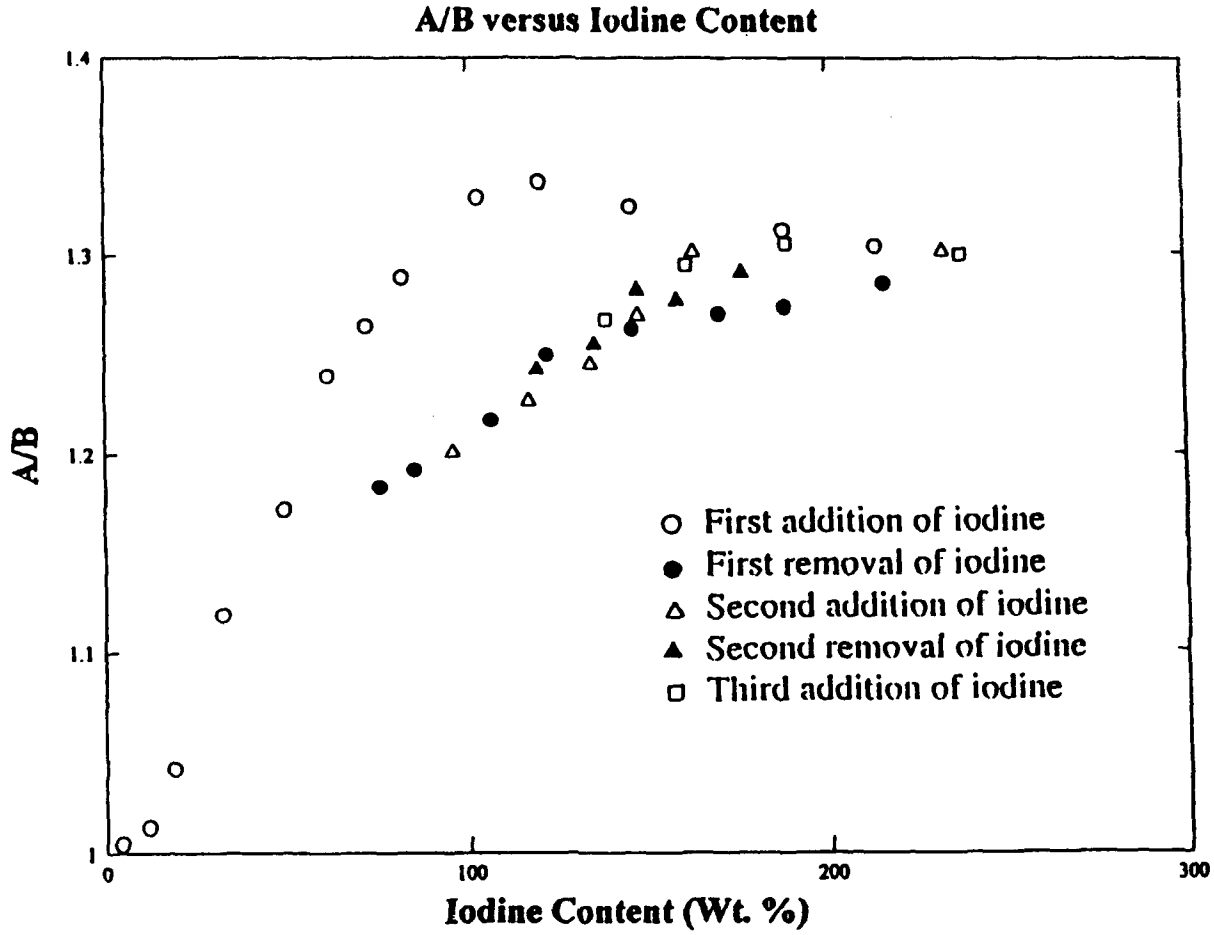

Figure 11. A plot of the asymmetry parameter, A/B, versus iodine content for Thermcon 1000.

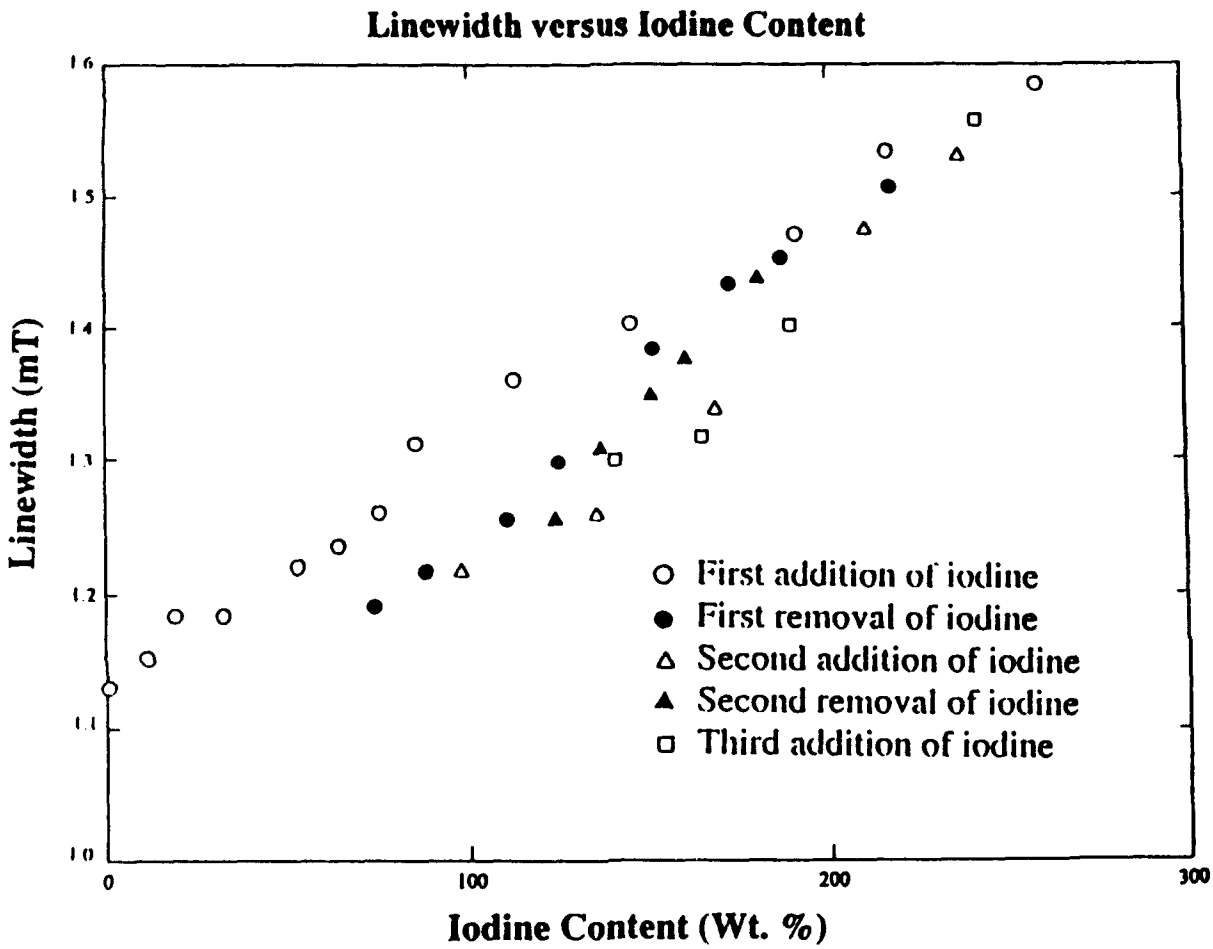

Figure 12. A plot of the ESR linewidth, ΔH, versus iodine content for Thermcon 1000.

Equilibria Scheme

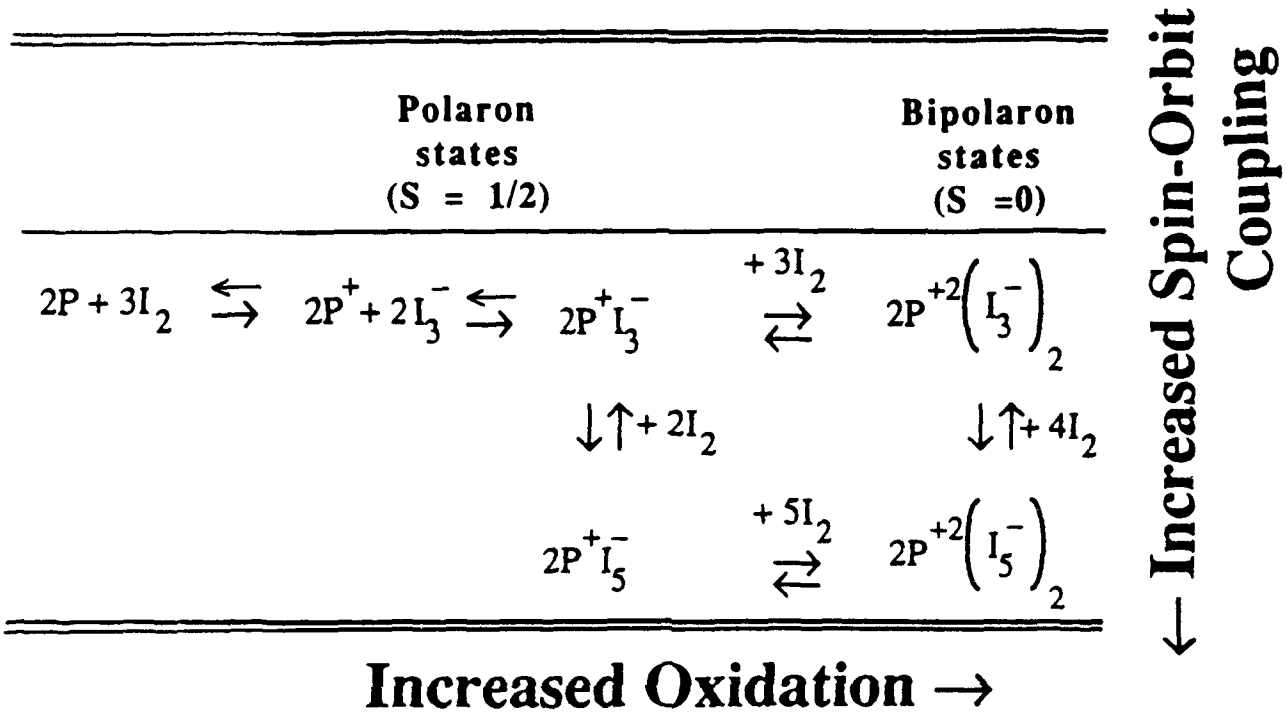

Figure 13. The equilibria scheme used to explain the dependences of the ESR lineshape parameters on iodine content.

radicals by way of the redox reaction with iodine. In the case of the DGEBA/DETA sample, the removal and addition of iodine shows that this radical formation is reversible. On the other hand, in the case of Thermcon 1000 with the first removal of iodine the radical concentration remains high, and in fact increases slightly with decreasing iodine content. However, following the first removal of iodine subsequent additions and removals shows that the formation of radicals is reversible. We can explain these behaviors in terms of the equilibria scheme outlined in Figure 13. According to this scheme, at high iodine concentrations both polarons and bipolarons can be present. As the iodine concentration is reduced the equilibrium will shift to the left, there will be a smaller number of bipolarons and the magnetic susceptibility will increase. Thus, the slight decrease in susceptibility measured in Thermcon 1000 samples with increasing iodine content for

the second and third doping provides evidence, albeit slight, for the formation of bipolarons in Thermcon 1000. Furthermore, the reversibility of radical formation in the DGEBA/DETA samples indicates that the equilibrium never proceeds beyond the first column in Figure 13, and bipolarons are not formed in this polymer.

The value of <g> depends on the principal values of the g-tensor averaged over all directions, whereas the values of A/B and ΔH are determined by g-anisotropy and to a lesser extent by the homogeneous packet width. Thus, the typical lineshapes that can be expected by assuming an axial g-tensor with the g-anisotropy $(g_{||} - g_{\perp}) = 0.015$ and $(g_{||} - g_{\perp}) = 0.005$ are shown in Figure 13, where $g_{||}$ is the g-value when the external field is along the axial direction and $g_{\perp}$ is the g-value when the external field is perpendicular to the axial direction. To a good approximation $\langle g \rangle = (g_{||} + g_{\perp})/2$, whereas the values of A/B and ΔH are determined by the $(g_{||} - g_{\perp})$ values, i.e., the g-anisotropy. One can therefore expect increases in the A/B value to be accompanied by increases in the ΔH value.

As is shown in Figures 10, 11 and 12, when the iodine content is increased from 0 to 300 wt% all the lineshape parameters (both in Thermcon 1000 and DGEBA/DETA epoxy) increase with iodine content. After the first undoping all show reversible behavior on subsequent doping and undoping. However, the lineshape parameter data also show that the values obtained on the first addition and first removal are different. We infer that this difference is the result of an irreversible chemical reaction of the iodine with the polymer. The values of the lineshape parameters obtained on subsequent addition and subtractions are related to this "iodinated" form of the polymer.

The preliminary data show that the reversible and irreversible behaviors of the Thermcon 1000 and DGEBA/DETA epoxy lineshape parameters on the addition and removal of iodine appear to be the same, and only differ in degree. Thus, the background radicals present in Thermcon 1000 after curing play no major role in changing the behavior of the lineshape parameters with increasing iodine content. These background radicals are probably perturbed by

the iodine in the same way as the redox radicals, so that the measured values of the lineshape parameters are an average value for the two radicals. This would account for the slight differences in behavior for Thermcon 1000 and the DGEBA/DETA thermosets.

The increase in <g> value with increasing iodine content can be explained qualitatively in terms of of an increase in the relative number of radical species with the higher iodine stoichiometry (i.e., $P^+I_5^-$ shown in the equilibria model depicted in Figure 13) and hence larger spin-orbit couplings. As predicted, increases in the A/B values are usually accompanied by increases in ΔH values. We conclude that these increases in the A/B and ΔH values with increasing iodine content imply an increasing g-anisotropy (i.e., the ($g_{\|} - g_{\perp}$) value) with increasing iodine content. In terms of the equilibria model in Figure 13, this conclusion implies that the $P^+I_5^-$ complex has a higher g-anisotropy than the $P^+I_3^-$ complex.

Temperature Dependence of the Lineshape Parameters: Measurements of the values of the lineshape parameters <g>, A/B and ΔH were also made at 77 K. The results summarized in Table 1 indicate a decrease in the <g> value ($\approx (g_{\perp} + g_{\|})/2$) as well as an increase in the A/B and ΔH values with decreasing temperature for all samples. The latter implies that the g-anisotropy increases with decreasing temperature. As is shown in Table 1, samples with low iodine contents exhibit smaller changes in the lineshape parameters on lowering the temperature than samples with high iodine content but both show the same temperature dependent trends.

Table 1. Temperature Dependence of ESR Lineshape Parameters.

Matrix	Temperature (K)	Linewidth (mT)	A/B	<g>	Iodine Content (wt%)
Thermcon 1000	300	1.59	1.32	2.0052	235
	77	1.65	1.43	2.0045	235
	300	1.35	1.2	2.0044	141
	77	1.43	1.27	2.0043	141
DGEBA/DETA	300	1.20	1.45	2.0053	264
	77	1.30	1.58	2.0046	264
	300	0.83	1.28	2.0040	159
	77	0.83	1.29	2.0037	159
DGEBA/DDH	300	1.13	1.45	2.0051	395
	77	1.35	1.68	2.0046	395
Error		±0.05	±0.01	±0.00005	

The temperature dependence of <g> can also be explained qualitatively in terms of the equilibria model depicted in Figure 13. The decrease in <g> with decreasing temperature implies that the complex with lowest spin-orbit interactions, and hence lowest iodine stoichiometry, viz., $P^+I_3^-$, lies lower in energy than the $P^+I_5^-$ complex.

The observed increase in the g-anisotropy with decreasing temperature is more difficult to explain. As was concluded from the room temperature data, the $P^+I_5^-$ has more g-anisotropy than the $P^+I_3^-$ complex. Moreover, since the temperature dependence of <g> suggests an increase of the $P^+I_3^-$ concentration with decreasing temperature, one would expect to observe a decrease of the g-anisotropy with decreasing temperature. One possible explanation involves a motional averaging of the g-anisotropy (but not the <g>value) at room temperature. If this motion is "frozen out" at 77 K, it would account for the increase in g-anisotropy with decreasing temperature. Two types of motion are possible: fast translational motion of the spins down polymer chains in the network or localized motions close to the spins. This fast translational motion down polymer chains seems unlikely in the amine-cured epoxy polymers, DGEBA/DETA and DGEBA/DDH, because of the lack of extended conjugation.

3.2 AT- Polyaniline Studies

During 1993-1994, our AT-polyaniline studies focused on the following four objectives:

(1) Improve the conductivity in the ATPA-7 materials by oxidizing them with O_2 or with $(NH_4)_2S_2O_3$.

(2) Prepare polyaniline-type oligomers having modified chemical structures that would cause them to have lower melting points than the original poly(para-phenyleneamineimine) type aniline octamers studied in 1992-1993.

(3) Make the doped ATPA-7 materials more processable (lower melting) and more thermally stable by doping them with different sulfonic acids.

(4) Continue the characterization of selected ATPA-7 samples using NMR and gel permeation chromotography (GPC).

3.2.1 Polyaniline Samples With High Oxidation States

Our results in 1992-1993 demonstrated that a modified Manassen-Khalif (MK) Schiff base approach[7] was more practical than the Modified Honzl-Wudl (MH-W) method[8,9] for the synthesis of ATPA-7. Work during 1993-1994 has shown that the ATPA-7 and the related poly(p-phenyleneamineimine) prepared by the MK method (PPAI-MK) exist mostly in the leuco form but can be oxidized to the emeraldine-base form which gives the maximum conductivity upon doping. The structures for the different oxidation states of PPAI are shown in Figure 14.

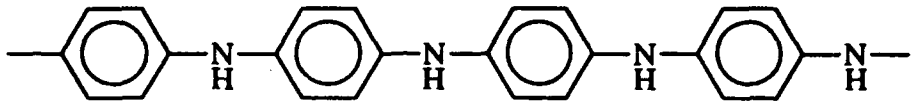

Leucoemeraldine

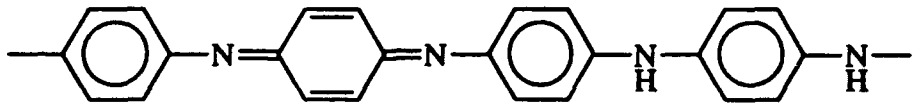

Emeraldine Base

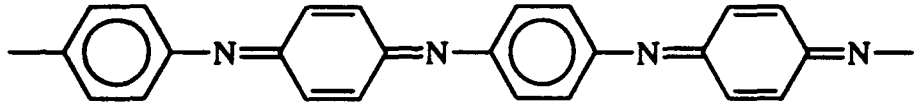

Pernigraniline

Figure 14. The structures of the typical polyaniline-type material in different oxidation states, viz., leucoemeraldine, emeraldine-base and pernigraniline.

This effort has involved the synthesis of PPAI and ATPA-7 oligomers using the MK approach,[7] and their subsequent oxidation to the emeraldine-base form as well as their reduction to the leuco form. Oxidation was achieved by bubbling O_2 into solutions of the oligomer or polymer as well as treating the solutions with $(NH_4)_2S_2O_3$. The structures of the PPAI and the ATPA-7 oligomers are shown in Figure 15.

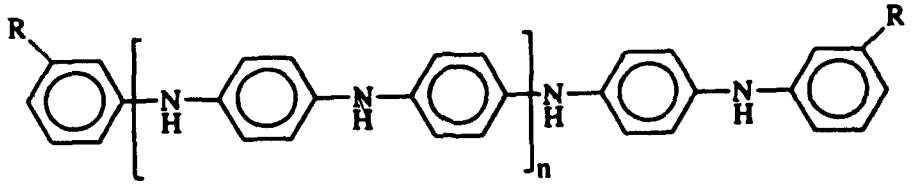

PPAI (R = H; n=large)
ATPA-7 (R = C≡CH; n=3)

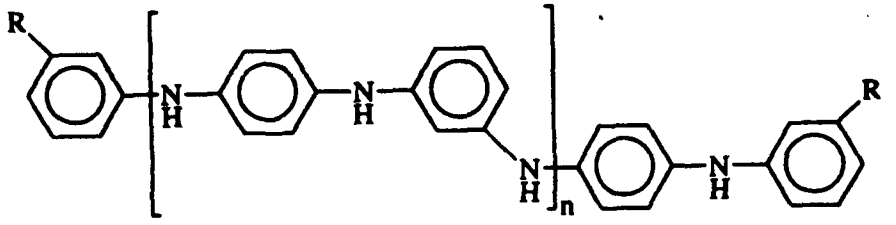

m,p-PPAI (R = H; n=large)
m,p-ATPA-7 (R = C≡CH; n=3)

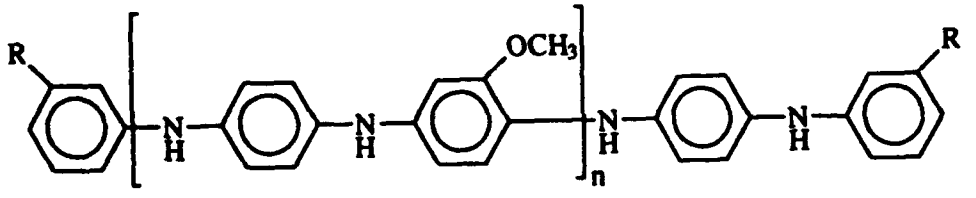

MeO-PPAI (R = H; n=large)
MeO-ATPA-7 (R = C≡CH; n=3)

(aniline-co-anisidine)

Figure 15. The substituted oligomers of PPAI and ATPA-7 that are being studied.

Synthesis and Oxidation of ATPA-7: The modified MK synthesis used to prepare ATPA-7 involved the reaction of 1,4-phenylenediamine with 1,4-cyclohexanedione (CHD) in m-cresol at 65-70°C for 72 h in an argon atmosphere followed by the addition of an excess of m-ethynylaniline (EA). The reaction was continued for an additional 96 hours before exposure to the atmosphere for periods up to 22 h. After the usual work-up the product was obtained as a gray powder. Yields ranged between 43-53%. The FTIR spectra obtained using KBr mulls and the UV-vis spectra determined using dilute solutions in N,N-dimethylformamide (DMF) indicated that the product ATPA-7 exists mostly in the leuco form. The FTIR spectrum shows an intensity ratio of 1/4 for the azaquinoid/benzenoid absorptions. A dilute DMF solution is pale blue and the UV-vis spectrum has absorptions at 328 nm and 600 nm with an intensity ratio of 15.

When molecular oxygen was bubbled into DMF solutions of samples of ATPA-7 at room temperature up to 22 h there was an increase in blue color and a dramatic increase in the intensity of the UV-vis absorption at 600 nm. The samples were worked up by pouring into 1 N HCl solution, collecting the dark green precipitate, treating it on the filter with 7 N NH_4OH, filtering, and washing with water until the washes were neutral to pH paper. The dark blue solid obtained after drying gave an IR spectrum with an intensity ratio of 1/2 for the azaquinoid (1597 cm^{-1}) to benzenoid (1505 cm^{-1}) absorptions. The UV-vis spectrum showed absorptions at 322 nm and 610 nm with an intensity ratio that had decreased to 3. This decrease confirms the conversion of the leuco form of ATPA-7 to the emeraldine-base form as a result of oxidation with oxygen. As is shown in Table 2, the corresponding electrical conductivities of the HCl doped samples increased from 9×10^{-5} to 1×10^{-3} S/cm but the values were markedly lower than that reported for polyaniline (5 S/cm).

Table 2. Doping and Conductivity of ATPA-7 Derivatives.

Sample	Doping	Conductivity (S/cm)
ATPA-7--no O_2	0.1 M HCl--m&p	9×10^{-5}
	0.1 M HCl--ppt	7×10^{-4}
ATPA-7--with O_2	0.1 M HCl--m&p	1×10^{-3}
	0.1 M HCl--ppt	5×10^{-4}
MeO-ATPA-7	0.1 M HCl--m&p	$<10^{-11}$
m,p-ATPA-7	0.1 M HCl--m&p	4×10^{-8}

Note: Samples were doped either by reprecipitation from NMP or DMF solution, 'ppt', or were doped by grinding in a mortar while covered with doping solution (m&p). In both cases the concentrations are indicated in the table, i.e., 0.1 M.

The molecular weight distribution was determined by gel permeation chromatography (GPC) using tetrahydrofuran (THF) solutions of samples of ATPA-7 before and after treatment with oxygen. The results showed that there is no change in molecular weight distribution as a result of the oxidation. Both samples gave virtually identical broad range molecular weight distributions (7000-500) with the largest fraction occurring in the higher molecular weight range. The ^1H NMR spectrum (in d_6 DMF) showed the presence of alkyl protons (ca 2 ppm, broad multiplet), acetylenic protons (4 ppm), and aromatic protons (7 ppm).

A sample of ATPA-7 sample was reduced to enhance its solubility for NMR experiments, and to provide a baseline UV-vis spectrum for use in assessing the degree of oxidation of the ATPA-7 samples. The phenylhydrazine reduction of ATPA-7 gave leuco ATPA-7 as a light gray solid. A dilute DMF solution was colorless and, as shown in Figure 16, exhibited a UV-vis spectrum with an absorption at 322 nm only. The azaquinoid absorption at 1597 cm^{-1} in the IR spectrum was absent, being replaced by the benzene ring absorption at 1601 cm^{-1}. After 17 h treatment with oxygen, this DMF solution turns blue with UV-vis absorptions at 325 nm and 615 nm (Intensity ratio = 3) indicating a conversion to the emeraldine-base form. Examples of the UV-vis spectra are shown in Figure 16.

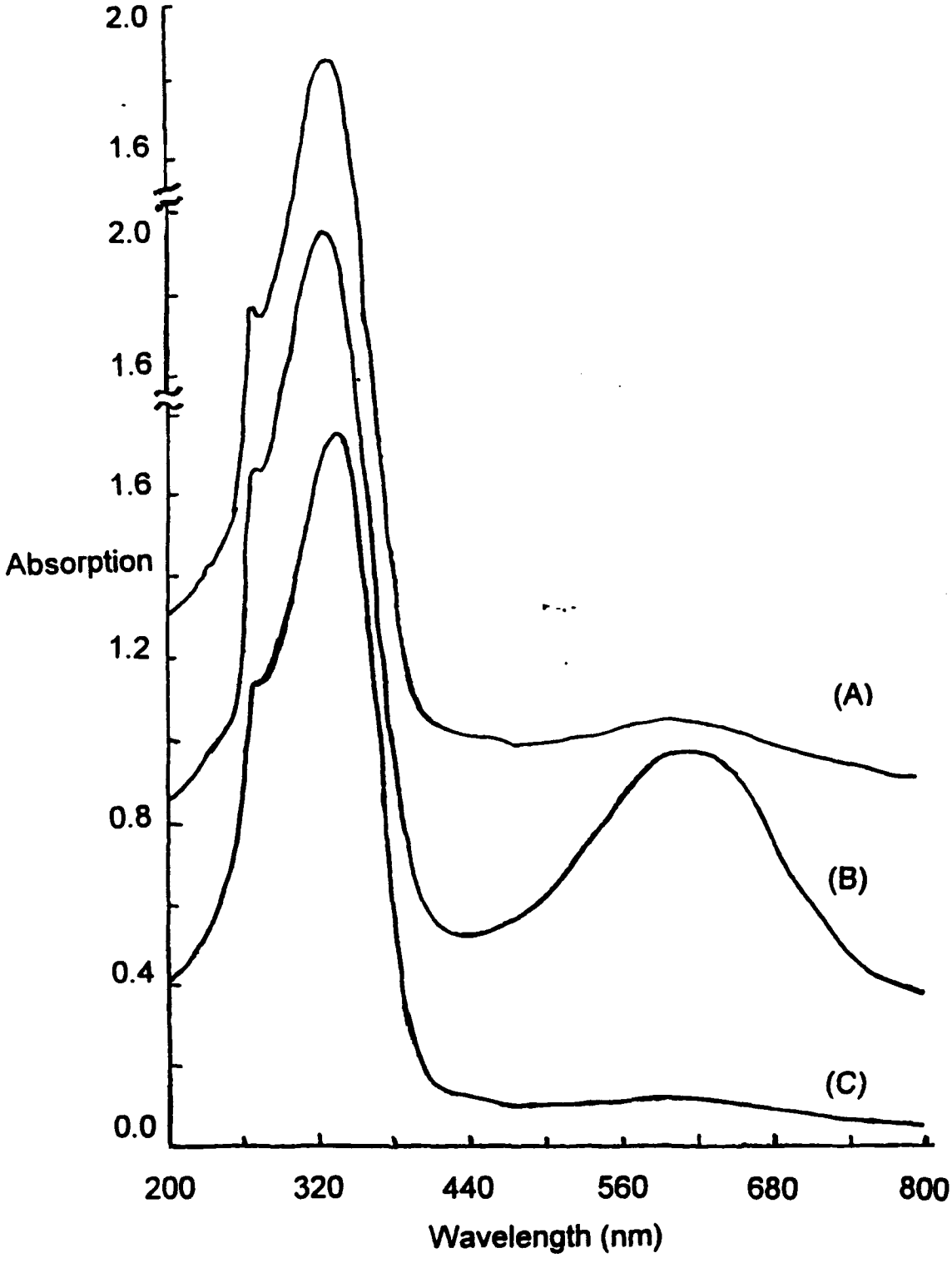

Figure 16. UV-vis spectra of ATPA-7 (A) as synthesized, (B) following oxidation with oxygen, and (C) following reduction with phenylhydrazine.

The GPC results, which are shown in Figure 17, indicate a wide molecular weight distribution (100 to 7000) and most notably a significant increase in the lower molecular weight fraction at 1200 and 1000 following the reduction with phenylhydrazine. This could be due to degradation of chains due to carbon-nitrogen bond cleavage during the reduction with phenylhydrazine (24 h at 115°C).

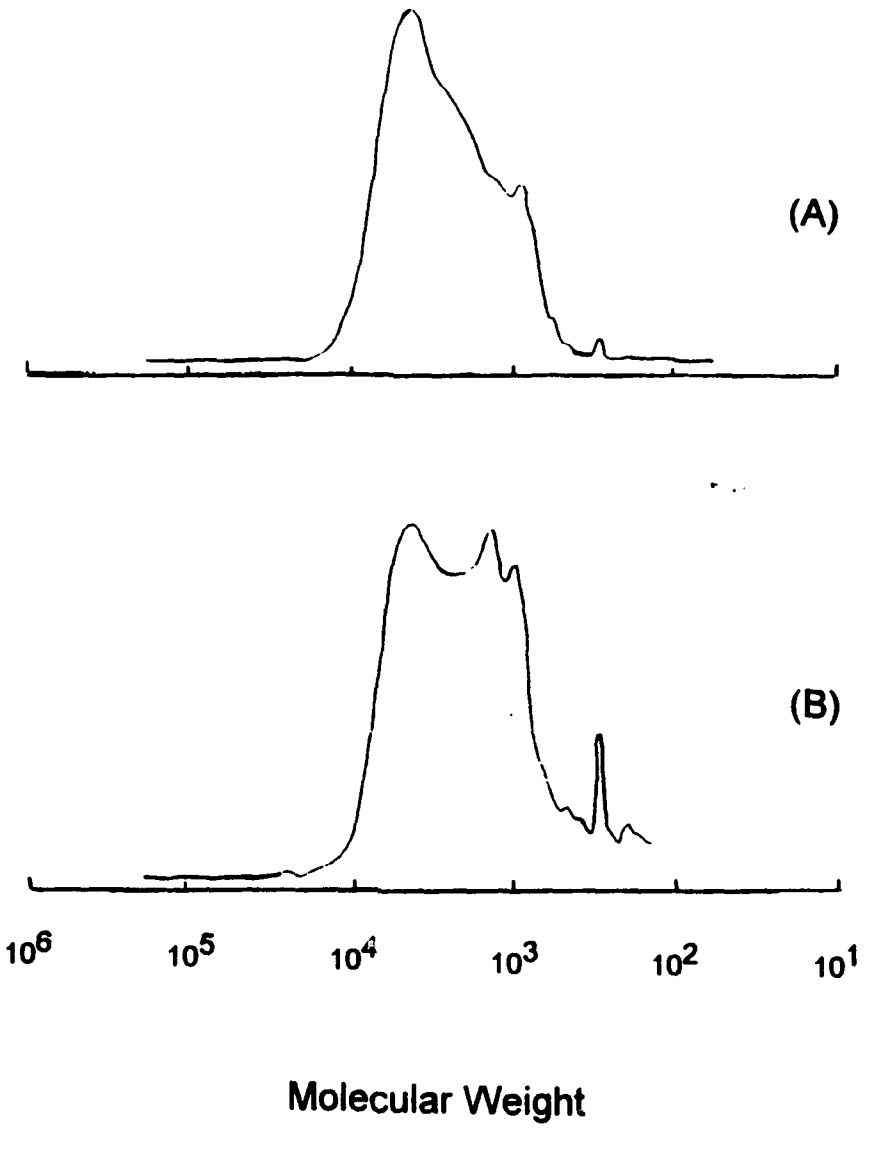

Figure 17. GPC chromatograms from ATPA-7 in THF prior to and following reduction using phenylhydrazine: (A) before reduction and (B) after reduction.

Synthesis and Oxidation of PPAI-MK: Comparison of PPAI prepared by the MK method with PPAI prepared by the MH-W method indicates that the MK method gives mostly the leuco form. Unlike the MH-W synthesis, a tan precipitate does not form during the MK synthesis until the reaction mixture has been exposed to the atmosphere for about 2 h whereupon a dark gray color begins to form. The PPAI-MK product is obtained in highest yield (88%) when molecular oxygen is bubbled into the m-cresol reaction mixture at 68°C for 22 h after the tan precipitate has formed. However, the product obtained in this case or by the usual 22 h exposure to the atmosphere is largely leuco PPAI as indicated by FTIR and UV-vis spectra.

The emeraldine-base form of PPAI was obtained with further oxidation by bubbling molecular oxygen into a stirred DMF solution for 22 h at room temperature. The FTIR spectrum shows an azaquinoid (1593 cm^{-1}) to benzenoid (1497 cm^{-1}) absorption ratio of 1/2. The color of the DMF solution becomes dark blue and the UV-vis spectrum has absorptions at 327 nm and 617 nm with an intensity ratio of 2.6. As shown in Table 3, the maximum electrical conductivity measured in an HCl doped sample of PPAI was 2×10^{-2} S/cm, which is also markedly lower than that usually reported in polyaniline (5 S/cm).

Table 3. Doping and Conductivity of Polyaniline (PPAI-MK) Derivatives

Sample	Doping	Conductivity (S/cm)
PPAI--no O_2	1 M HCl--ppt	not measured
PPAI--with O_2	1 M HCl--ppt	2×10^{-2}
m,p-PPAI	0.1 M HCl--m&p	3×10^{-7}
MeO-PPAI	0.1 M HCl--m&p	1×10^{-9}

Note: Samples were doped either by reprecipitation from NMP or DMF solution, 'ppt', or were doped by grinding in a mortar while covered with doping solution (m&p). In both cases the HCl concentrations are indicated on the table (0.1 M or 1.0 M HCl).

Oxidation of PPAI by a solution of ammonium persulfate in 1 N HCl for 22 h at room temperature also gave the emeraldine base form of PPAI after the usual work-up. The FTIR and

UV-vis spectra of this PPAI in solution are essentially identical to the spectra of the emeraldine base form of PPAI produced by oxidation with molecular oxygen. The dark blue DMF solution gave a UV-vis spectrum with absorption at 327 nm and 613 nm (the intensity ratio = 2.4). The FTIR spectrum had an azaquinoid (1597 cm^{-1}) to benzenoid (1498 cm^{-1}) absorption ratio of 1/2.

3.2.2 Modified Polyaniline Oligomers With Improved Processability

We have attempted to improve the processability (i.e., lowered melting and curing temperatures) of the ATPAs by introducing alkoxy substituents and using meta substitution to produce irregularity in the backbones. The structures of these oligomers are shown in Figure 15.

Synthesis and conductivity of m,p-polyaniline (m,p-PPAI): This polymer as well as its structurally similar octamer (m,p-ATPA-7, see below) were synthesized using a modified MK method. We have investigated the effect of meta substitution on the conductivity of m,p-PPAI by comparing its conductivity with that measured in polyaniline (i.e., 5 S/cm). A quantitative yield of product was obtained as a dark solid which consisted of two fractions, one that was very soluble in N-methylpyrrolidine (NMP) and another that was slightly soluble. Both were oxidatively treated with a solution of ammonium persulfate in 1 N HCl. The UV-vis spectra of the fraction slightly soluble in NMP lacked absorption in the azaquinoid region (600 nm). Samples were doped with 0.1 M HCl in 95% H_2O/5% ethanol and, as shown in Table 3, the conductivities were found to be 3 x 10^{-7} S/cm which is significantly less than the value measured in para-polyaniline prepared using the MK method (PPAI-MK) (i.e., 2 x 10^{-2} S/cm).

Synthesis of m,p-ATPA-7: This was obtained as a dark brown solid in 51% yield. The IR spectrum is similar to that of ATPA-7 and confirms the presence of N-H, C=C-H, some ketone carbonyl, and aliphatic C-H groups. It also showed two bands around 1617 and 1487 cm^{-1}. A dilute DMF solution is pale yellow, and the 600 nm azaquinoid absorption is absent in the UV-vis spectrum. The UV-vis spectrum of a sample in DMF that was treated with oxygen gas at room temperature for 20 h was unchanged. Unlike ATPA-7, m,p-ATPA-7 apparently resists further oxidation under these conditions. A doped sample which was prepared

as a dark green solid precipitate by pouring this DMF solution into 1 N HCl, gave a conductivity value 4.0 x 10^{-8} S/cm. (See Table 2.)

Synthesis of Methoxyl-Substituted ATPA-7: This oligomer (MeO-ATPA-7) was obtained in 62% yield as a black powder. Since it is more soluble in acetone and methanol than other ATPA-7s, it may prove to be more solvent processible. The IR spectrum supported the proposed structure and indicated the presence of N-H, C=C-H, CH_3O (2923 cm^{-1}), azaquinoid (1606 and 1599 cm^{-1}), and benzenoid (1502 cm^{-1}) groups as well as the absence of carbonyl groups. A dilute solution in DMF was a light purple color, and the UV-vis spectrum exhibited absorptions at 284 and 513 nm. Acidification with concentrated HCl caused a bathochromic shift to 581 nm but no color change. This is in contrast to the larger shift that occurs when a DMF solution of ATPA-7 is acidified with HCl, to produce a color change from blue to green. A sample of this material was further oxidized by bubbling oxygen gas into the DMF solution maintained at 70°C for 19 h. Precipitation from 1 N HCl solution afforded a black powder that was soluble in methanol. A dilute DMF solution of this powder was light purple with absorptions at 283 and 496 nm. Acidification resulted in formation of a pale green-black color and a bathochromic shift to 595 nm. The long-wavelength absorption at 513 nm before oxidation and at 496 nm thereafter, suggests that the MeO-ATPA-7 has significant pernigraniline structure, which is known to absorb in the 500-540 nm region and is purple. For MeO-ATPA-7 this is not surprising, since the 2-methoxy-1,4-diaminobenzene is expected to be more easily oxidized than unsubstituted p-phenylenediamine. A sample of HCl-doped, methoxy-substituted polyaniline polymer (MeO-PPAI), poly(aniline-co-anisidine), was tested for conductivity, and found to have a value of only 1 x 10^{-9} S/cm. This was much lower than the values measured in either unsubstituted ATPA-7 or PPAI (See Tables 2 and 3). Moreover, Pandey et al.,[10] have reported a conductivity value of ~10^{-4} S/cm for a random copolymer of aniline and anisidine.

3.2.3 Alternative Dopants for Improved Processability and Thermal Stability

In order to improve the processability (i.e., low melting samples) and thermal stability relative to that observed for typical HCl doped polyaniline samples, we have doped selected samples with camphorsulfonic acid (CSA), dodecylbenzenesulfonic acid (DBSA), and benzenedisulfonic acid (BDSA).

Doping with CSA: Two ATPA-7 samples were doped with CSA. In one case, a powdered sample was exposed to a 0.2 M solution of CSA in 95% water, 5% ethanol solution, whereas in the second case an ATPA-7 sample was dissolved in NMP, then precipitated by pouring this solution into 0.2 M CSA. Both samples were pressed into disks and their conductivities measured. The samples doped as a powder were hard, while the samples doped by precipitation were soft. On heating to 150°C they became and remained soft enough for the spring loaded conductivity probes to penetrate their surface. This soft samples had higher conductivities than the sample doped as a powder. As can be seen from Table 4, the conductivity for these samples drops rapidly within the first hour of cure at 150°C.

Table 4. Conductivity of ATPA-7 Doped with Camphor Sulfonic Acid vs. Cure Time

Sample	Time at 150°C (min)	Conductivity (S/cm)
Doped by Reprecipitation:	0	n/a -- too soft
	25	1.2×10^{-6}
	54	4.5×10^{-9}
	129	10^{-7} to 10^{-4}*
	1200	6×10^{-10}
Doped as Powder in Mortar and Pestle	0	n/a -- too soft
	25	1.2×10^{-7}
	54	6×10^{-8}
	1200	$\sim 10^{-11}$

* Sample conductivity increased dramatically with room humidity and probe penetration.

Doping with DBSA: According to MacDiarmid et al.,[11] it is possible to dope polyaniline with dodecylbenzene sulfonic acid (DBSA) and cast these samples from xylene to obtain conductivities as high as 20 S/cm. We have attempted to obtain highly conductive samples using this approach. The procedure followed involved dissolving a sample in xylene containing 40% DBSA, followed by heating to 100°C for 1 day to drive off xylene. This left a gelatinous material which was subsequently titrated with water to leave a filterable solid. The solid was finally rinsed with 0.2 N DBSA and dried. In a pellet of PPAI-MK that had been oxidized with $(NH_4)_2S_2O_3$ the conductivity was only 2×10^{-4} S/cm, whereas in a pellet of PPAI-MK that had been doped with HCl the value was 1×10^{-3} S /cm.

Doping with BDSA: According to the patent literature[12] polyaniline containing BDSA as a dopant remains stable at 150°C for 48 h. The BDSA was acquired in the form of its disodium salt (80% purity; the material also contained 20% sodium sulfate). Successful conversion to the free acid was accomplished by use of an ion exchange column having sulfonic acid functionality. The resulting BDSA contained a 20% sulfuric acid contaminant. We used this BDSA/H_2SO_4 mixture to dope a sample of ATPA-7. The ATPA-7 was first dissolved in NMP, then precipitated into an aqueous solution of the dopant. Following filteration and air drying for 24 h, the doped ATPA-7 remained a swollen gel. This sample was placed in a 150°C oven, and its conductivity and hardness were monitored as a function of time. The results are shown in Table 5.

Table 5. Resistance of an ATPA-7 Sample Doped With Benzenedisulfonic Acid vs Cure Time.

Time at 150°C (min)	Resistance (ohms)	Nature of Sample
0	1.5×10^4	swollen gel
20	1.5×10^4	melt/viscous liquid
50	3×10^6	soft at 150°C, hard at 20°C
110	$>4 \times 10^9$	very hard solid

Despite its lower conductivity upon heat treatment, the BDSA doped ATPA-7 sample showed very good curing behavior: Following a 2 h cure at 150°C, the sample changed from being a processable gel to a very hard solid that could be pulverized with a mortar and pestle only with difficulty. In contrast, the typical uncured powders can be pulverized with relative ease.

3.2.4 Characterization of Selected Oligomer samples by NMR and GPC

NMR experiments : In this study two questions were addressed: (1) What was the degree of polymerization of a typical ATPA-7 sample? and (2) Did the spectrum indicate complete aromatization of the sample? A typical result is shown in Figure 18, where a spectrum of reduced phenyl-capped octaaniline (COA), can be compared with a spectrum of reduced ATPA-7, which has acetylene group terminations. A comparison of these two spectra indicates that the acetylenic hydrogen peak occurs at 4.0 ppm. Moreover, the area of this peak (8 units) with the area of the aromatic region (125 units) leads us to conclude a degree of polymerization (DP) of 28. An explanation for this high DP may be that partial reduction of the acetylene groups may have occurred. Both the COA and ATPA-7 NMR spectra have peaks in the aliphatic region, indicating that these materials are not fully aromatized. This could explain the low conductivities we have observed for the ATPA-7 and PPAI-MK samples.

GPC Analysis: Two types of GPC data were taken. The first type consisted of ATPA or COA dissolved in THF. The second type consisted of ATPA or COA dissolved in a 5% solution of di-n-butylamine (DNBA) in THF to break up clusters of oligomer that might form. The results of both types of experiments were the same. Figure 17 shows typical data acquired for ATPA-7 in THF, whereas Figure 19 shows typical data for ATPA-7 in DNBA/THF. In both cases the molecular weights are uncorrected values, referenced to polystyrene standards. Figure 19 indicates that ATPA-7 oligomers have (uncorrected) molecular weights that range from 500 to 7500. This distribution yields a number-average molecular weight (Mn) of ~1270, and weight-average molecular weight (Mw) of ~5000. Average molecular weight values calculated

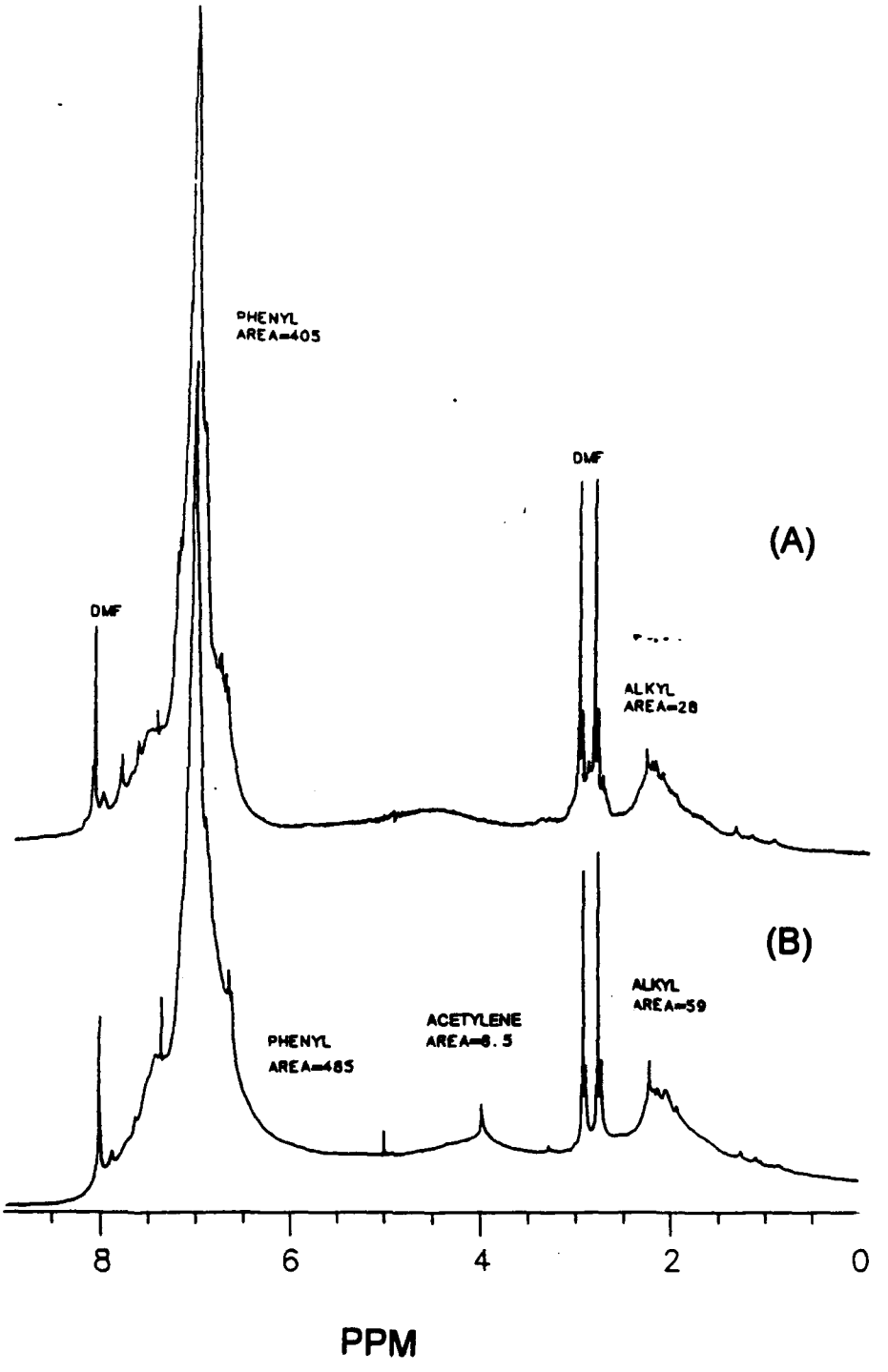

Figure 18. ^{1}H NMR spectra of COA and ATPA-7 both following reduction with phenylhydrazine: (A) COA and (B) ATPA-7.

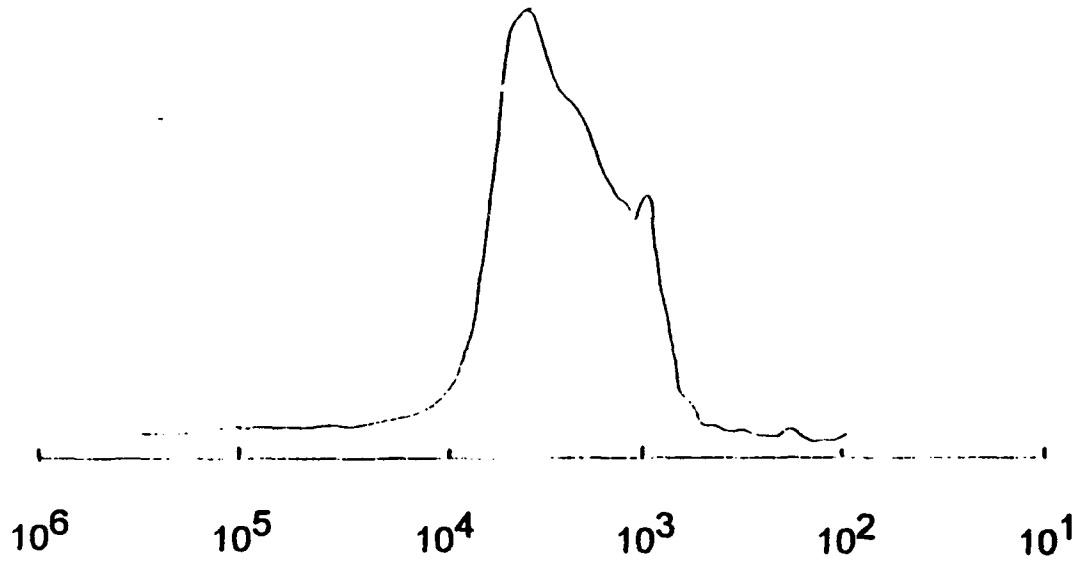

Figure 19. GPC chromatogram for ATPA-7 in 5 % DNBA/THF solution.

from three separate ATPA-7 samples are: Mn = ~1250 and Mw = ~4550. These values appear to be consistent with those expected from the stoichiometry used in the synthesis, which was adjusted to yield a nominal Mn value of ~900. The value derived from the NMR data, viz., Mn = 2550, DP = 28, is higher, but could be artificially high because of the possible partial reduction of the acetylenic groups mentioned above.

4.0 WORK TO BE DONE IN 1994-1995 PERIOD

In the 1994-1995 period we will we will continue our work on thermosets made from AT-polyaniline oligomers, and AT-polythiophene monomers and oligomers. We will also extend our studies to acetylene-terminated phenylenevinylenes which are analogues for the AT-Schiff bases as well as monomers terminated with phenylacetylene. On curing, the latter should form thermosets which have smaller crosslink densities. In the AT-polyaniline work we are confident that the MK method is a reliable procedure for synthesizing the PPAI and ATPA-7

substituted derivatives. However, we do not fully understand why the conductivities measured in these materials are two or more orders of magnitude lower than the value reported for bulk polyaniline. We will make additional efforts to understand the reasons for these low values so that we can improve the electrical performance of these materials. For example, we will use electrochemical techniques to investigate further the oxidation of selected oligomers to see how complete is the formation of the emeraldine-base states which are necessary for high conductivity.

5.0 MDA-E PERSONNEL AND SUBCONTRACTORS

Former MDA-E Personnel:

I. M. Brown, Principal Investigator (presently at University of Missouri-St.Louis)

D. J. Leopold (presently at Washington University)

T. C. Sandreczki (presently at University of Missouri-Kansas City)

Subcontractor

Southwest Missouri State University:

S. Mohite

J. Wilbur

6.0 REFERENCES

1. J. M. Pickard, E. G. Jones, and I. J. Goldfarb, "Kinetics and Mechanism of the Bulk Thermal Polymerization of (3-Phenoxyphenyl) Acetylene", Macromolecules 12, 895 (1979).
2. "Conducting Thermoset Polymers: A Comparative Study of Schiff Base Precursors With Different End-Groups". Manuscript written and will be submitted to Synthetic Metals.
3. "Conducting Thermoset Polymers," Annual Technical Report, 30 September 1993, AFOSR Contract No. F49620-92-C-0074, MDC 93B0476.

4. P. Chicart, R. J. P. Corriu, J. J., Moreau , F. Garnier and A. Yassar, "Selective Synthetic Routes to Electroconductive Organosilicon Polymers Containing Thiophene Units," Chem. Mater. 3, 8 (1991).

5. We have used four different schemes to synthesize in small quantities the four thiophene compounds shown in Figure 4, but outline here only the scheme used in the synthesis of 3T-2AT.

6. T. C. Sandreczki and C. Y. C. Lee, "Characterization of Acetylene-Terminated Resin Cure States Using EPR Spectroscopy," Polymer Preprints 23, (2), 185 (1982).

7. J. Manassen and S. Khalif, "Organic Polymers, Correlation Between Their Structures and Catalytic Activity in Heterogeneous Systems," J. Am. Chem. Soc., 88, 1943 (1966).

8. J. Honzl and M. Tlustakova, "Polyaniline Compounds. II. The Linear Oligoaniline Derivatives Tri-, Tetra-, and Hexaanilineobenzene and Their Conductive Complexes," J. Polym. Sci., Part C, 22, 451 (1968).

9. F. Wudl, R. O. Angus, F. L. Lu, P. M. Allemand, D. J. Vachon, M. Nowak, Z. X. Liu and A. J. Heeger, "Poly(p-Phenyleneamineimine: Synthesis and Comparison to Polyaniline," J. Am. Chem. Soc. 109, 3677 (1987).

10. S. S. Pandey, S. Annapoorni, and B. D. Malhotra, "Synthesis and Characterization of Poly(aniline-co-o-anisidine): A Processible Conducting Polymer," Macromolecules 26, 3190 (1993).

11. H. L. Wang and A. G. MacDiarmid, "Polyaniline: Secondary Doping in the Dodecylbenzenesulfonic Acid System," Bull. Am. Phys. Soc. 39, 426 (1994).

12. R. E. Cameron, "High Service Temperature Conductive Polymers and Method of Producing Same," International Patent Application Number PCT/US89/03131, International Publication Number WO 90/01775, 22 February 1990, LockheedCorporation.